Structural Engineering and Mechanics, *Vol. 58, No. 3 (2016) 423-442*
DOI: http://dx.doi.org/10.12989/sem.2016.58.3.423

Axisymmetric analysis of a functionally graded layer resting on elastic substrate

Muhittin Turan[a], Gokhan Adiyaman[*], Volkan Kahya[b] and Ahmet Birinci[c]

Department of Civil Engineering, Karadeniz Technical University, 61080, Trabzon, Turkey

(Received October 12, 2015, Revised January 18, 2016, Accepted February 5, 2016)

Abstract. This study considers a functionally graded (FG) elastic layer resting on homogeneous elastic substrate under axisymmetric static loading. The shear modulus of the FG layer is assumed to vary in an exponential form through the thickness. In solution, the FG layer is approximated into a multilayered medium consisting of thin homogeneous sublayers. Stiffness matrices for a typical homogeneous isotropic elastic layer and a half-space are first obtained by solving the axisymmetric elasticity equations with the aid of Hankel's transform. Global stiffness matrix is, then, assembled by considering the continuity conditions at the interfaces. Numerical results for the displacements and the stresses are obtained and compared with those of the classical elasticity and the finite element solutions. According to the results of the study, the approach employed here is accurate and efficient for elasto-static problems of FGMs.

Keywords: stiffness matrix method; functionally graded material; layered media; elasticity; Hankel's transform

1. Introduction

Functionally graded material (FGM) is the special type of composite whose composition varies continuously as a function of position along thickness or length of a structure. In design of FGM, the microstructure is gradually varied from one material to another with a specific gradient. This enables the material to have good specifications of both materials in its composition. The concept of FGM has been first introduced in Japan in 1980s. Aircrafts, space vehicles, defense industries, electronics and biomedical sensors are some application areas of FGMs in engineering.

Many engineering structures or materials can be considered as multilayered bodies. For example, a soil could be idealized as a set of linear elastic or viscoelastic layers of infinite and horizontal extent. Composite materials can also be considered as layered anisotropic structures in some cases. In the analysis of multilayered media, the elasticity problem for all layers must be solved. These solutions must also satisfy the boundary and continuity conditions. Consequently, the classical method for multilayered media is required to solve a system of simultaneous

*Corresponding author, Research Assistant, E-mail: gadiyaman@ktu.edu.tr
[a]Research Assistant, E-mail: m.turan@ktu.edu.tr
[b]Associate Professor, E-mail: volkan@ktu.edu.tr
[c]Professor, E-mail: birinci@ktu.edu.tr

http://www.techno-press.org/?journal=sem&subpage=8 ISSN: 1225-4568 (Print), 1598-6217 (Online)

equations with a large number of unknown constants. The complexity of such a solution can be found in the studies of Iyengar and Alwar (1964), Chen (1971), in which the semi-infinite medium consisting of isotropic layers was considered, as well as that of Pagano (1970) for the problem of anisotropic laminates in cylindrical bending.

An axi-symmetric frictionless contact for a transversely isotropic functionally graded elastic half-space resting on a rigid base with a small axisymmetric surface recess was investigated by Barik *et al*. (2009). The problem was reduced to Fredholm integral equations, and solved numerically. Rhimi *et al*. (2011) considered the axisymmetric problem of a frictionless double receding contact between a rigid stamp of axisymmetric profile, a functionally graded layer and a homogeneous half space. The problem is solved by the theory of elasticity and an appropriate integral transform. The axisymmetric torsional problem of functionally graded layer located between a homogenous layer and homogenous half plane was solved by Liu *et al*. (2015) using the Hankel integral transform. It is assumed that the shear modulus of the graded layer changed exponentially along the thickness direction and the homogenous layer was loaded by a rigid cylindrical punch. Oner *et al*. (2015) presented a comparative study for a continuous contact problem by analytical and finite element method (FEM).

Alternatively, various solution procedures have been developed for the analysis of layered media based on matrix analysis. Among them, the transfer matrix method was developed by Bufler (1971), and independently by Bahar (1972). Small and Booker (1984, 1986) introduced an exact finite layer flexibility matrix for the analysis of horizontally layered elastic material. They solved the static problem of layered media under strip, circular, and rectangular loading cases. Choi and Thangjitham (1991) performed the stress analysis of multilayered anisotropic elastic media subjected to applied surface tractions by the stiffness matrix method. They also studied the steady-state thermoelasticity problem of a layered anisotropic medium under the state of generalized plane deformation (1991). Pindera and Lane (1993) studied the frictionless contact problem of layered half-planes consisting of arbitrary number of isotropic, orthotropic, or monoclinic layers arranged in any sequence by the stiffness matrix method. Wang and Ishikawa (2001) proposed a method for the linear elasto-static analysis of multilayered bodies by the matrix analysis. By using the transfer matrix approach, Sun and Luo (2008), Sun *et al*. (2009) studied transient and steady-state wave propagation in multilayered viscoelastic media. Sun *et al*. (2013) proposed a high-order thin layer method to improve accuracy and robustness of the thin layer method for analyzing viscoelastic wave propagation in stratified media. An exact stiffness method for quasi-static analysis of multilayered poroelastic media was proposed by Senhjuntichai and Rajapakse (1995). Ai and co-workers (2011, 2012) developed an analytical layer-element method for solutions to axisymmetric and non-axisymmetric consolidation problems of multilayered soils. Ai and Wang (2015) presented an analytical layer-element solution to axisymmetric thermal consolidation of multilayered porous thermoelastic media containing a deep buried heat source. Recently, based on the analytical layer-element solution of the axisymmetric problem of multilayered isotropic soils, Ai and Cai (2015) presented a theory for static analysis of a Timoshenko beam on elastic multilayered isotropic soils by combination of finite element and analytical layer element.

As an alternative to the classical elasticity solution, this study attempts to solve elasto-static problem of a functionally graded (FG) elastic layer resting on homogeneous elastic substrate subjected to axisymmetric static loading by the stiffness matrix method. The shear modulus of the FG layer is assumed to vary in an exponential form through the thickness. In solution, the FG layer is approximated into a multilayered medium consisting of thin homogeneous sublayers. For each sublayer, the shear modulus is calculated at its midplane, and is assumed to be constant through the

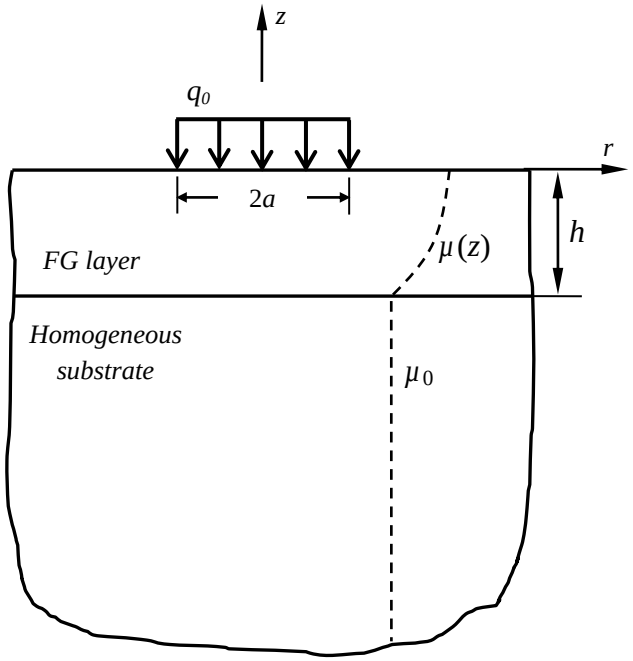

Fig. 1 Geometry and loading of the problem

thickness. Stiffness matrices for the homogeneous isotropic elastic layer and the half-space are first obtained by solving axisymmetric elasticity equations with the aid of Hankel's transform. Global stiffness matrix is, then, assembled by considering the continuity conditions at the interfaces. Numerical results for displacements and stresses are obtained and compared with those of the classical elasticity and the finite element solutions. Results show that the present approach for elasto-static problem of FG bodies is accurate, and can be used as an alternative method for problems including FGMs.

2. Governing equations and general solutions

Fig. 1 shows geometry and the loading of the problem considered. Since the loading applied on the medium is axisymmetric, it is convenient to use the cylindrical coordinate system (r,θ,z) for the formulation. In the absence of body forces, the equilibrium equations for a homogeneous isotropic elastic material can be given as

$$\frac{\partial \sigma_r}{\partial r} + \frac{\partial \tau_{rz}}{\partial z} + \frac{\sigma_r - \sigma_\theta}{r} = 0,$$
$$\frac{\partial \tau_{rz}}{\partial r} + \frac{\partial \sigma_z}{\partial z} + \frac{\tau_{rz}}{r} = 0 \tag{1}$$

where σ_r, σ_θ and τ_{rz} are the stress components shown in Fig. 2.

The displacement-strain relationships are given by

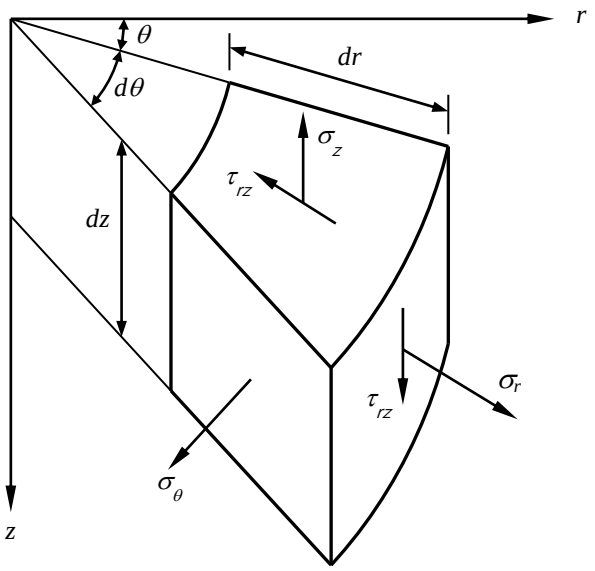

Fig. 2 Stress components in the cylindrical coordinate system

$$\varepsilon_r = \frac{\partial u_r}{\partial r}, \quad \varepsilon_\theta = \frac{u_r}{r}, \quad \varepsilon_z = \frac{\partial u_z}{\partial z}, \quad \gamma_{rz} = \frac{\partial u_r}{\partial z} + \frac{\partial u_z}{\partial r}, \quad \gamma_{r\theta} = \gamma_{\theta z} = 0 \tag{2}$$

where $u_r=u_r(r,z)$ and $u_z=u_z(r,z)$ are the displacement components in radial and vertical directions, respectively.

The stress-strain relationship can be given by

$$\boldsymbol{\sigma} = \mathbf{C}\boldsymbol{\varepsilon} \tag{3}$$

or explicitly

$$\begin{Bmatrix} \sigma_r \\ \sigma_\theta \\ \sigma_z \\ \tau_{\theta z} \\ \tau_{rz} \\ \tau_{r\theta} \end{Bmatrix} = \begin{bmatrix} \lambda+2\mu & \lambda & \lambda & 0 & 0 & 0 \\ \lambda & \lambda+2\mu & \lambda & 0 & 0 & 0 \\ \lambda & \lambda & \lambda+2\mu & 0 & 0 & 0 \\ 0 & 0 & 0 & \mu & 0 & 0 \\ 0 & 0 & 0 & 0 & \mu & 0 \\ 0 & 0 & 0 & 0 & 0 & \mu \end{bmatrix} \begin{Bmatrix} \varepsilon_r \\ \varepsilon_\theta \\ \varepsilon_z \\ \gamma_{\theta z} \\ \gamma_{rz} \\ \gamma_{r\theta} \end{Bmatrix} \tag{4}$$

where $\lambda=Ev/[(1+v)(1-2v)]$ and $\mu=E/[2(1+v)]$ are Lamé elastic constants in which E and v are Young's modulus and Poisson's ratio, respectively.

Substituting Eq. (2) into Eq. (4) yields the stress-displacement relations as

$$\sigma_r = \lambda\Delta + 2\mu\frac{\partial u_r}{\partial r}, \qquad \sigma_\theta = \lambda\Delta + 2\mu\frac{u_r}{r}, \qquad \sigma_z = \lambda\Delta + 2\mu\frac{\partial u_z}{\partial z},$$
$$\tau_{rz} = \mu\left(\frac{\partial u_r}{\partial z} + \frac{\partial u_z}{\partial r}\right), \quad \tau_{r\theta} = \tau_{\theta z} = 0 \tag{5a-f}$$

where $\Delta=(\partial u_r/\partial_r)+(u_r/r)+(\partial u_z/\partial z)$.

Substituting Eq. (5) into Eq. (1) gives the equations of equilibrium in terms of displacements, i.e., Navier equations, as

$$(\lambda+2\mu)\left(\frac{\partial\Delta}{\partial r}-\frac{u_r}{r^2}\right)+\mu\frac{\partial}{\partial z}\left(\frac{\partial u_r}{\partial z}-\frac{\partial u_z}{\partial r}\right)=0,$$
$$(\lambda+2\mu)\frac{\partial\Delta}{\partial z}+\mu\left(\frac{\partial}{\partial r}+\frac{1}{r}\right)\left(\frac{\partial u_z}{\partial r}-\frac{\partial u_r}{\partial z}\right)=0 \quad \text{(6a, b)}$$

Solution to Eq. (6) can be obtained by the integral transform method. Let's define *n*th order Hankel's transform of a function $f(r)$ and its inversion as

$$\bar{f}(s)=\int_0^\infty f(r)J_n(sr)r\,dr,$$
$$f(r)=\int_0^\infty \bar{f}(s)J_n(sr)s\,ds \quad \text{(7a, b)}$$

where s is the transform variable corresponding to the radial coordinate r, and J_n is the Bessel function of the first kind of order n.

Applying Hankel's transform of order 1 to Eq. (6a), and applying Hankel's transform of order 0 to Eq. (6b), one may obtain

$$(\lambda+2\mu)\left(-s^2\bar{u}_r-s\frac{\partial\bar{u}_z}{\partial z}\right)+\mu\left(\frac{\partial^2\bar{u}_r}{\partial z^2}+s\frac{\partial\bar{u}_z}{\partial z}\right)=0,$$
$$(\lambda+2\mu)\left(s\frac{\partial\bar{u}_r}{\partial z}+\frac{\partial^2\bar{u}_z}{\partial z^2}\right)+\mu\left(-s^2\bar{u}_z-s\frac{\partial\bar{u}_r}{\partial z}\right)=0 \quad (9)$$

or in matrix form

$$\begin{bmatrix}\mu & 0\\ 0 & \lambda+2\mu\end{bmatrix}\begin{Bmatrix}\bar{u}_r''\\ \bar{u}_z''\end{Bmatrix}+\begin{bmatrix}0 & -s(\lambda+\mu)\\ s(\lambda+\mu) & 0\end{bmatrix}\begin{Bmatrix}\bar{u}_r'\\ \bar{u}_z'\end{Bmatrix}+\begin{bmatrix}-s^2(\lambda+2\mu) & 0\\ 0 & -s^2\mu\end{bmatrix}\begin{Bmatrix}\bar{u}_r\\ \bar{u}_z\end{Bmatrix}=\begin{Bmatrix}0\\ 0\end{Bmatrix} \quad (10)$$

where primes denote the derivatives with respect to z. Assuming $\bar{u}_r(s,z)=u_{r0}e^{ksz}$ and $\bar{u}_z(s,z)=u_{z0}e^{ksz}$, and substituting them into Eq. (10) gives

$$\begin{bmatrix}\lambda+\mu(2-k^2) & (\lambda+\mu)k\\ (\lambda+\mu)k & -\mu+(\lambda+2\mu)k^2\end{bmatrix}\begin{Bmatrix}\bar{u}_{r0}\\ \bar{u}_{z0}\end{Bmatrix}=\begin{Bmatrix}0\\ 0\end{Bmatrix} \quad (11)$$

The linear algebraic equation system in Eq. (11) has non-trivial solutions when determinant of its coefficient matrix equals zero. This gives the following

$$k^4-2k^2+1=0 \quad (12)$$

which has roots $k_1=k_2=1$, and $k_3=k_4=-1$. Thus, the solutions of $\bar{u}_r(s,z)$ and $\bar{u}_z(s,z)$ become

$$\bar{u}_r(s,z)=(A_1+A_2z)e^{sz}+(B_1+B_2z)e^{-sz} \quad (13)$$

$$\bar{u}_z(s,z) = (C_1 + C_2 z)e^{sz} + (D_1 + D_2 z)e^{-sz} \tag{14}$$

where A_i, B_i, C_i and D_i (i=1,2) are unknown coefficients to be determined from boundary conditions of the problem. Inserting Eqs. (13) and (14) into any of Eqs. (9), the unknown coefficients C_i and D_i can be expressed in terms of A_i and B_i, respectively. Thus, we have

$$\bar{u}_r(s,z) = (A_1 + A_2 z)\cosh sz + (B_1 + B_2 z)\sinh sz \tag{15}$$

$$\bar{u}_z(s,z) = (-B_1 + \frac{R}{s}A_2 - B_2 z)\cosh sz + (-A_1 + \frac{R}{s}B_2 - A_2 z)\sinh sz \tag{16}$$

where R=(λ+3μ)/(λ+μ).

Apply Hankel's transform of order 0 to Eqs. (5a-c), and apply Hankel's transform of order 1 to Eqs. (5d-f) to obtain the stresses for a typical kth layer. For the stress components of the layer, this transformation gives

$$\bar{\sigma}_z(s,z) = (\lambda + 2\mu)\frac{\partial \bar{u}_z}{\partial z} + \lambda s\bar{u}_r, \quad \bar{\tau}_{rz}(s,z) = \mu\left(\frac{\partial \bar{u}_r}{\partial z} - s\bar{u}_z\right) \tag{17}$$

Substituting Eqs. (15) and (16) into Eqs. (17) yields

$$\bar{\sigma}_z(s,z) = \left[-2\mu s(A_1 + A_2 z) + \chi B_2\right]\cosh sz + \left[-2\mu s(B_1 + B_2 z) + \chi A_2\right]\sinh sz \tag{18}$$

$$\bar{\tau}_{rz}(s,z) = \mu\left[2s(B_1 + B_2 z) - (R-1)A_2\right]\cosh sz + \mu\left[2s(A_1 + A_2 z) - (R-1)B_2\right]\sinh sz \tag{19}$$

where χ=(λ+2μ)(R−1).

For a semi-infinite layered medium with the Nth layer modeled as a half-space, the regularity conditions are imposed such that the transformed displacements satisfy $\bar{u}_r(s,-\infty) \to 0$ and $\bar{u}_z(s,-\infty) \to 0$. To ensure these conditions, the coefficients of the exponential term e^{-sz} in Eqs. (13) and (14) must be zero. Thus, we have

$$\bar{u}_r(s,z) = (A_1 + A_2 z)e^{|s|z} \tag{20}$$

$$\bar{u}_z(s,z) = (C_1 + C_2 z)e^{|s|z} \tag{21}$$

Substituting Eqs. (20) and (21) into any of Eqs. (9) to express unknown coefficients C_i and D_i in terms of A_i and B_i, respectively, yields

$$\bar{u}_r(s,z) = (A_1 + A_2 z)e^{|s|z} \tag{22}$$

$$\bar{u}_z(s,z) = \mathrm{sgn}(s)\left(-A_1 + \frac{R}{|s|}A_2 - A_2 z\right)e^{|s|z} \tag{23}$$

Substituting Eqs. (22) and (23) into Eqs. (17) gives

$$\bar{\sigma}_z(s,z) = s\left[-2\mu(A_1 + A_2 z) + \frac{\chi}{|s|}A_2\right]e^{|s|z} \tag{24}$$

$$\bar{\tau}_{rz}(s,z) = \mu|s|\left[2A_1 - \left(\frac{R-1}{|s|} + 2z\right)A_2\right]e^{|s|z} \tag{25}$$

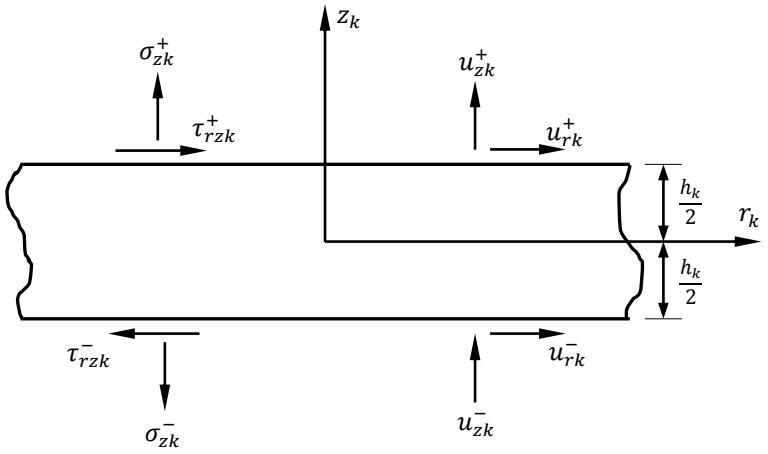

Fig. 3 Displacements and stresses at the upper and lower surfaces of the kth layer

3. Stiffness matrix method

As can be seen in the foregoing section, there are four unknown constants A_i and B_i (i=1,2) for each layer. Consequently, for an N-layer medium, a total of 4N unknown constants must be determined from a set of 4N appropriate boundary and interface conditions. This means that the classical method is required to solve a system of algebraic equations with a large number of unknowns. To overcome this difficulty, the stiffness matrix method is employed for the analysis. Fig. 3 shows the displacement and stress components at the upper and lower surfaces of the layer. Note that the local coordinate system for the kth layer is located at its middle. The signs (+) and (–) refer the values at upper and lower surfaces of the layer, respectively. Let's define the following vectors for a typical homogeneous isotropic kth layer within a multilayered medium.

$$\begin{aligned} \bar{\mathbf{d}}_k &= \left\{ \bar{u}_r^k \quad \bar{u}_z^k \right\}^T, \quad \bar{\boldsymbol{\sigma}}_k = \left\{ \bar{\sigma}_r^k \quad \bar{\sigma}_z^k \right\}^T, \\ \mathbf{a}_k &= \left\{ A_1^k \quad A_2^k \right\}^T, \quad \mathbf{b}_k = \left\{ B_1^k \quad B_2^k \right\}^T \end{aligned} \tag{26}$$

where $\bar{\mathbf{d}}_k(s,z)$ and $\bar{\boldsymbol{\sigma}}_k(s,z)$ are the vectors for the transformed displacements and stresses, respectively, and $\mathbf{a}_k(s)$ and $\mathbf{b}_k(s)$ are the vectors for the unknown constants.

In terms of $\mathbf{a}_k$ and $\mathbf{b}_k$, the vectors containing values of the transformed displacements $\bar{\mathbf{d}}_k^{\pm}$ and stresses $\bar{\boldsymbol{\sigma}}_k^{\pm}$ for the kth layer are expressed as

$$\begin{Bmatrix} \bar{\mathbf{d}}_k^+ \\ \bar{\mathbf{d}}_k^- \end{Bmatrix} = \begin{bmatrix} \mathbf{F}_{11}^k & \mathbf{F}_{12}^k \\ \mathbf{F}_{21}^k & \mathbf{F}_{22}^k \end{bmatrix} \begin{Bmatrix} \mathbf{a}_k \\ \mathbf{b}_k \end{Bmatrix} \tag{27}$$

$$\begin{Bmatrix} \bar{\boldsymbol{\sigma}}_k^+ \\ -\bar{\boldsymbol{\sigma}}_k^- \end{Bmatrix} = \begin{bmatrix} \mathbf{G}_{11}^k & \mathbf{G}_{12}^k \\ \mathbf{G}_{21}^k & \mathbf{G}_{22}^k \end{bmatrix} \begin{Bmatrix} \mathbf{a}_k \\ \mathbf{b}_k \end{Bmatrix} \tag{28}$$

where $\mathbf{F}_{ij}^k(s)$ and $\mathbf{G}_{ij}^k(s)$ (i=j=1, 2) are the 2×2 real submatrices. Eliminating the unknown vectors $\mathbf{a}_k$ and $\mathbf{b}_k$ from Eqs. (27) and (28), the surface stresses and displacements for the kth layer are

obtained as

$$\begin{Bmatrix} \bar{\boldsymbol{\sigma}}_k^+ \\ -\bar{\boldsymbol{\sigma}}_k^- \end{Bmatrix} = \begin{bmatrix} \mathbf{K}_{11}^k & \mathbf{K}_{12}^k \\ \mathbf{K}_{21}^k & \mathbf{K}_{22}^k \end{bmatrix} \begin{Bmatrix} \bar{\mathbf{d}}_k^+ \\ \bar{\mathbf{d}}_k^- \end{Bmatrix} \tag{29}$$

where $\mathbf{K}_{ij}^k(s)$ (i=j=1, 2) are the 2×2 real submatrices defined as

$$\begin{bmatrix} \mathbf{K}_{11}^k & \mathbf{K}_{12}^k \\ \mathbf{K}_{21}^k & \mathbf{K}_{22}^k \end{bmatrix} = \begin{bmatrix} \mathbf{G}_{11}^k & \mathbf{G}_{12}^k \\ \mathbf{G}_{21}^k & \mathbf{G}_{22}^k \end{bmatrix} \begin{bmatrix} \mathbf{F}_{11}^k & \mathbf{F}_{12}^k \\ \mathbf{F}_{21}^k & \mathbf{F}_{22}^k \end{bmatrix}^{-1} \tag{30}$$

where the left-hand side of the above equation is the 4×4 real and symmetric local stiffness matrix for the kth layer. The elements of the local stiffness matrix for a homogeneous isotropic layer are given in Appendix A in explicit form.

For an N-layer infinite solid subjected to tractions applied on the bounding surfaces, the boundary and interface continuity conditions between two adjacent layers are imposed such that

$$\begin{aligned} &\bar{\boldsymbol{\sigma}}_1^+ = \bar{\mathbf{p}}^+, \\ &\bar{\boldsymbol{\sigma}}_k^- = \bar{\boldsymbol{\sigma}}_{k+1}^+, \ \bar{\mathbf{d}}_k^- = \bar{\mathbf{d}}_{k+1}^+ \quad (k = 1, 2, \ldots, N-1), \\ &\bar{\boldsymbol{\sigma}}_N^- = \bar{\mathbf{p}}^- \end{aligned} \tag{31}$$

where $\mathbf{p}^{\pm}(s)$ denote the Hankel's transform of the applied tractions on the upper (+) and lower (–) bounding surfaces of the medium.

Defining $\bar{\boldsymbol{\delta}}_1 = \bar{\mathbf{d}}_1^+$ and $\bar{\boldsymbol{\delta}}_{N+1} = \bar{\mathbf{d}}_N^-$, the displacements vectors for the upper and lower bounding surface of the medium, respectively, and $\bar{\boldsymbol{\delta}}_{k+1} = \bar{\mathbf{d}}_k^- = \bar{\mathbf{d}}_{k+1}^+$ (k=1,2,3,...,N−1), the vectors containing values of the interfacial displacements common to the kth and (k+1)th layers, the following system of equations can be obtained through the successive applications of the conditions given in Eq. (31).

$$\begin{aligned} &\mathbf{K}_{11}^1 \bar{\boldsymbol{\delta}}_1 + \mathbf{K}_{12}^1 \bar{\boldsymbol{\delta}}_2 = \bar{\mathbf{p}}^+, \\ &\mathbf{K}_{21}^k \bar{\boldsymbol{\delta}}_k + (\mathbf{K}_{22}^k + \mathbf{K}_{11}^{k+1}) \bar{\boldsymbol{\delta}}_{k+1} + \mathbf{K}_{12}^{k+1} \bar{\boldsymbol{\delta}}_{k+2} = \mathbf{0} \quad (k = 1, 2, \ldots, N-1), \\ &\mathbf{K}_{21}^N \bar{\boldsymbol{\delta}}_N + \mathbf{K}_{22}^N \bar{\boldsymbol{\delta}}_{N+1} = \bar{\mathbf{p}}^- \end{aligned} \tag{32}$$

The above system of algebraic equations can be represented in the following matrix form

$$\begin{bmatrix} \mathbf{K}_{11}^1 & \mathbf{K}_{12}^1 & 0 & \cdot & \cdot \\ \mathbf{K}_{21}^1 & \mathbf{K}_{22}^1 + \mathbf{K}_{11}^2 & \mathbf{K}_{12}^2 & \cdot & \cdot \\ 0 & \mathbf{K}_{21}^2 & \mathbf{K}_{22}^2 + \mathbf{K}_{11}^3 & \cdot & \cdot \\ 0 & 0 & \mathbf{K}_{21}^3 & \cdot & \cdot \\ 0 & 0 & 0 & \cdot & \mathbf{K}_{22}^N \end{bmatrix} \begin{Bmatrix} \bar{\boldsymbol{\delta}}_1 \\ \bar{\boldsymbol{\delta}}_2 \\ \cdot \\ \cdot \\ \bar{\boldsymbol{\delta}}_{N+1} \end{Bmatrix} = \begin{Bmatrix} \bar{\mathbf{p}}_1^+ \\ 0 \\ \cdot \\ 0 \\ \bar{\mathbf{p}}_N^- \end{Bmatrix} \tag{33}$$

or shortly

$$\mathbf{K}\bar{\boldsymbol{\delta}} = \bar{\mathbf{f}} \tag{34}$$

It is observed that the assembly of the global stiffness matrix for the entire medium is carried out

by superposing the local stiffness matrices of the individual layers along the main diagonal of the global matrix in an overlapping fashion. Dimension of the global stiffness matrix $\mathbf{K}(s)$ is $2(N+1)\times 2(N+1)$, the global displacement vector $\bar{\boldsymbol{\delta}}(s)$ is $2(N+1)\times 1$, and the global force vector $\bar{\mathbf{f}}(s)$ is $2(N+1)\times 1$, respectively.

For a semi-infinite layered medium in which the last layer is modeled as a homogeneous half-space, the local stiffness matrix equation of the half-space becomes

$$\bar{\boldsymbol{\sigma}}_N^+ = \hat{\mathbf{K}}_{11}^N \bar{\mathbf{d}}_N^+ \tag{35}$$

since $\bar{\boldsymbol{\sigma}}_N^- \to 0$ and $\bar{\mathbf{d}}_N^- \to 0$ when $z \to -\infty$. In Eq. (35), $\hat{\mathbf{K}}_{11}^N$ represents the local stiffness matrix for the half-space, of which dimension is 2×2. The elements of the local stiffness matrix for each homogeneous isotropic half-space are given in Appendix B in explicit form. Here, the local coordinate system is considered to be located on the top surface of the half-space, i.e., z_N=0. Thus, for a semi-infinite layered medium, the last submatrix of Eq. (33) is replaced by $\mathbf{K}_{22}^{N-1} + \hat{\mathbf{K}}_{11}^N$. In this case, the last subvector of the global interfacial displacement vector becomes $\bar{\boldsymbol{\delta}}_N$, and $\bar{\mathbf{p}}_N^-$ is zero. Thus, the dimension of the global stiffness matrix becomes $2N\times 2N$.

The general solution procedure of the stiffness matrix method can be summarized as:

(1) Solve the global interfacial displacement vector $\bar{\boldsymbol{\delta}}$ by Eq. (34);

(2) Calculate the transformed stresses $\bar{\boldsymbol{\sigma}}_k^{\pm}$ at the top and bottom surfaces of each layer by Eq. (29); and

(3) Calculate the real displacements $\boldsymbol{\delta}_k(r,z)$ and stresses $\boldsymbol{\sigma}_k(r,z)$ within the medium by taking the inverse Hankel's transform given by Eq. (7b).

4. Classical axisymmetric elasticity solution

In Section 2, general expressions for field variables of the homogeneous isotropic bodies were given. Following is the classical solution of the governing equations when considering gradual variation of elastic moduli within solid, i.e., FGM. For the FG layer, the material is assumed as non-homogeneous isotropic with a gradient along z-direction. The Poisson's ratio is assumed to be constant. The shear modulus of the layer varies along the z-direction, and is given by an exponential function as

$$\mu(z) = \mu_0 e^{\beta z}, \quad -h \le z < 0 \tag{36}$$

where μ_0 is the shear modulus of the homogeneous substrate, and β is the non-homogeneity parameter that controls the variation of the shear modulus within the FG layer.

For a FG medium, the governing differential equations given by Eq. (6) can be re-arranged when considering the variation of elastic moduli with z-direction as follows:

$$\begin{aligned}
&(\kappa+1)\left(\frac{\partial\Delta}{\partial r} - \frac{u_r}{r^2}\right) + (\kappa-1)\frac{\partial}{\partial z}\left(\frac{\partial u_r}{\partial z} - \frac{\partial u_z}{\partial r}\right) + (\kappa-1)\beta\left(\frac{\partial u_r}{\partial z} + \frac{\partial u_z}{\partial r}\right) = 0,\\
&(\kappa+1)\frac{\partial\Delta}{\partial z} - (\kappa-1)\left(\frac{\partial}{\partial r} - \frac{1}{r}\right)\left(\frac{\partial u_r}{\partial z} - \frac{\partial u_z}{\partial r}\right) + (3-\kappa)\beta\left(\frac{\partial u_r}{\partial r} + \frac{u_r}{r}\right) + (\kappa+1)\beta\frac{\partial u_z}{\partial z} = 0
\end{aligned} \tag{37}$$

where κ=3−4ν.

Eq. (37) must be solved under the following boundary conditions

$$\sigma_z^{(1)}(r,0) = -q_0 \quad r \le a, \quad \sigma_z^{(1)}(r,0) = 0 \quad r > a, \quad \tau_{rz}^{(1)}(r,0) = 0,$$
$$\sigma_z^{(1)}(r,-h) = \sigma_z^{(2)}(r,-h), \quad \tau_{rz}^{(1)}(r,-h) = \tau_{rz}^{(2)}(r,-h), \tag{38}$$
$$\frac{\partial}{\partial r}[u_z^{(1)}(r,-h)] = \frac{\partial}{\partial r}[u_z^{(2)}(r,-h)], \quad \frac{\partial}{\partial r}[u_r^{(1)}(r,-h)] = \frac{\partial}{\partial r}[u_r^{(2)}(r,-h)]$$

where q_0 is the uniform distributed load over the top surface of the layer, superscripts (1) and (2) denote the layer and the half-space, respectively.

Applying Hankel's transform to Eq. (37), and following the similar way described in Sec. 2, one may write the transformed displacements for the layer and the half-space as

$$\bar{u}_r^{(1)}(s,z) = \sum_{j=1}^{4} A_j(s) e^{n_j(s)z}, \qquad \bar{u}_z^{(1)}(s,z) = \sum_{j=1}^{4} A_j(s) m_j(s) e^{n_j(s)z} \tag{39a,b}$$

$$\bar{u}_r^{(2)}(s,z) = \left[B_1(s) + B_2(s)z\right] e^{sz}, \quad \bar{u}_z^{(2)}(s,z) = \left[-B_1(s) + \left(\frac{\kappa_2}{s} - z\right) B_2(s)\right] e^{sz} \tag{40a,b}$$

where

$$m_j = \frac{\left(3\beta + 2n_j - \beta\kappa_1\right)\left[n_j\left(\beta + n_j\right)\left(\kappa_1 + 1\right) - s^2\left(\kappa_1 + 3\right)\right]}{s\left[4s^2 - \beta^2\left(\kappa_1 - 3\right)\left(\kappa_1 + 1\right)\right]} \tag{41}$$

The unknown functions $A_j(s)$ (j=1,...,4), $B_1(s)$ and $B_2(s)$ in Eq. (40) are determined by the boundary conditions given in Eq. (38). $n_j(s)$ (j=1,...,4) are the complex roots of

$$n_j^4 + 2\beta n_j^3 + (\beta^2 - 2s^2) n_j^2 - 2s^2 \beta n_j + s^2 (s^2 + \beta^2 \frac{3 - \kappa_1}{\kappa_1 + 1}) = 0 \tag{42}$$

from which

$$n_{1,2} = -\frac{1}{2}\left(\beta \pm \sqrt{4s^2 + \beta^2 - 4s\beta i\sqrt{\frac{3-\kappa_1}{\kappa_1+1}}}\right), \quad n_{3,4} = -\frac{1}{2}\left(\beta \pm \sqrt{4s^2 + \beta^2 + 4s\beta i\sqrt{\frac{3-\kappa_1}{\kappa_1+1}}}\right) \tag{43}$$

Substituting Eqs. (39) and (40) into Eq. (17), and applying the inverse transform, the displacements and stresses can be obtained as follows:

(a) For the FG layer

$$\sigma_z^{(1)} = \frac{\mu(z)}{\left(\kappa_1 - 1\right)} \int_0^\infty s\left[\sum_{j=1}^{4} A_j(s) C_j(s) e^{n_j(s)z}\right] J_0(sr)\, ds,$$

$$\tau_{rz}^{(1)} = \mu(z) \int_0^\infty s\left[\sum_{j=1}^{4} A_j(s) D_j(s) e^{n_j(s)z}\right] J_1(sr)\, ds,$$

$$u_r^{(1)} = \int_0^\infty s\left[\sum_{j=1}^{4} A_j e^{n_j(s)z}\right] J_1(rs) ds,$$

$$u_z^{(1)} = \int_0^\infty s\left[\sum_{j=1}^{4} A_j m_j(s) e^{n_j(s)z}\right] J_0(rs)ds \tag{44}$$

where

$$C_j = (3-\kappa_1)s + (\kappa_1+1)m_j(s)n_j(s), \quad D_j = n_j(s) - s\,m_j(s) \tag{45}$$

(b) For the half-space,

$$\begin{aligned}
\sigma_z^{(2)} &= \frac{\mu_0}{(\kappa_2-1)}\int_0^\infty s\left[(\kappa_2-1)(-2sB_1 + (\kappa_2+1)B_2 - 2szB_2)e^{sz}\right] J_0(sr)\,ds,\\
\tau_{rz}^{(2)} &= \mu_0\int_0^\infty s\left[(2sB_1 + (1-\kappa_2)B_2 + 2szB_2)e^{sz}\right] J_1(sr)\,ds,\\
u_r^{(2)} &= \int_0^\infty s\left[B_1 + B_2 z\right]e^{sz} J_1(rs)ds,\\
u_z^{(2)} &= \int_0^\infty s\left[-B_1 + \left(\frac{\kappa_2}{s} - z\right)B_2\right]e^{sz} J_0(rs)ds
\end{aligned} \tag{46}$$

5. Results and discussion

Some numerical results are given in the following to show the accuracy and efficiency of the present approach in elasto-static problems of FGMs. In solution of the problem by the stiffness matrix method, the FG layer is replaced by a layered medium consisting of *N*-homogeneous layer. Each layer in the system has its own elastic moduli, which is obtained by Eq. (36) at its midplane. Thus, we have an *N*-layer medium in which each sublayer has different elastic moduli which is constant through the thickness.

The load applied over the medium can be either concentrated, i.e., a/h=0.01, or uniformly distributed, i.e., a/h=0.1, 0.5, 1.0, and 2.0. For all cases, the resultant force $P=q_0\pi a^2$ is always kept the same. Shear modulus of the FG layer at z=0 and z=-h are defined as μ_U and $\mu_L=\mu_0$, respectively. Poison's ratio for the FG layer and the homogenous substrate are taken as ν=0.3. Note that all quantities are normalized as follows:

$$\mu_U/\mu_L, \quad a/h, \quad r/h, \quad z/h, \quad u_r/h, \quad u_z/h, \quad \sigma_z/q_0, \quad \tau_{rz}/q_0$$

Convergence study is first performed. In Table 1, non-dimensional vertical displacements (u_z/h) obtained from the present method for different discretization scenarios of the FG layer are compared to those of elasticity solution. a/h=0.10 and μ_U/μ_L=4.00, 2.00, 1.00, 0.50 and 0.25 are used. Note that μ_U/μ_L=1.00 means the layer is homogeneous. For this case, the relative error is less than 1%, and the increase in the number of sublayers has no effect on the results. For μ_U/μ_L>1.00, the shear modulus of the layer decreases from top to bottom. On the contrary, i.e., for μ_U/μ_L<1.00, the shear modulus increases from top to bottom. It can be clearly seen that when the number of sublayers increases, the results obtained for the FG layer converge to the exact ones with an error of acceptable order. For

Table 1 Convergence study for the non-dimensional displacements $(u_z/h)\times 10^{-3}$ (a/h=0.10)

μ_U/μ_L	z/h	Elasticity	Present					
			N=1	N=5	N=10	N=20	N=40	N=80
4.00	0	-0.796	-1.039	-0.802	-0.796	-0.798	-0.799	-0.800
	-1	-0.159	-0.087	-0.142	-0.150	-0.154	-0.156	-0.157
2.00	0	-1.308	-1.558	-1.325	-1.317	-1.316	-1.316	-1.316
	-1	-0.175	-0.131	-0.165	-0.169	-0.172	-0.173	-0.174
1.00	0	-2.228	-2.248	-2.248	-2.248	-2.248	-2.248	-2.248
	-1	-0.190	-0.189	-0.189	-0.190	-0.189	-0.189	-0.189
0.50	0	-3.902	-3.116	-3.890	-3.934	-3.941	-3.942	-3.942
	-1	-0.204	-0.263	-0.215	-0.209	-0.206	-0.205	-0.204
0.25	0	-6.979	-4.155	-6.837	-7.021	-7.047	-7.055	-7.055
	-1	-0.215	-0.350	-0.241	-0.228	-0.221	-0.218	-0.216

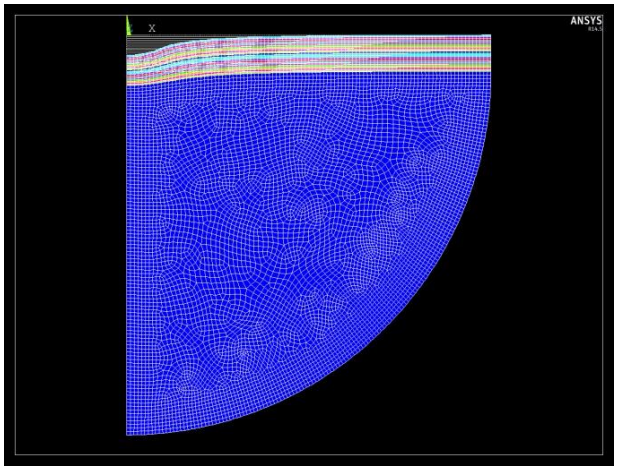

(a)

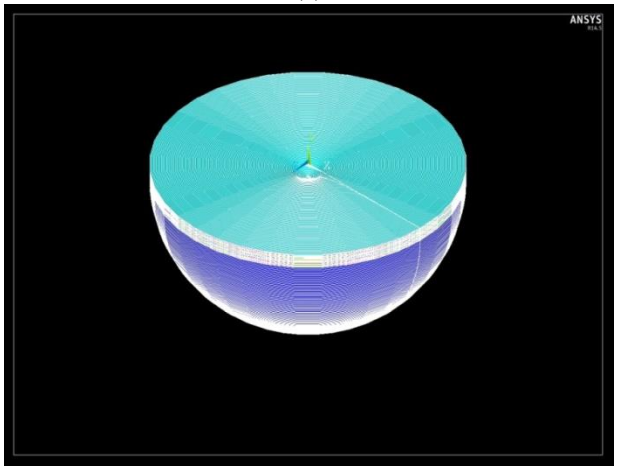

(b)

Fig. 5 Finite element model of the problem: Deformed shape for μ_U/μ_L=4.00 and a/h=1.00 (a) 2D view; (b) 3D view

N=20, the relative error is less than order of 3% for all μ_U/μ_L values. Therefore, for all analyses here, N=20 sublayers are selected for the discretization of the FG layer into N-layer medium.

For the aim of further comparison, the problem considered here is also solved by the finite element method (FEM) using the commercial FE software ANSYS. In FE modelling, only half of the problem is considered due to symmetry according to z-axis. PLANE183 axisymmetric solid element is used for FE meshing. Radial distance from the symmetry axis z is selected as 10 times the layer thickness, i.e., r/h=10. Mesh generation of the FG layer is made by manually while it is made automatically for the half-space. The material properties of the FG layer are assigned with the same way in discretizing the model by the stiffness matrix method. Note that for different a/h values, re-meshing of the FG layer is required. Fig. 5 shows an example of axisymmetric and 3D views of the FE model used in the analyses.

Table 2 Comparison of the non-dimensional normal stresses σ_z/q_0 for three methods considered (a/h=1.00)

z/h	μ_U/μ_L=0.25			μ_U/μ_L=1.00			μ_U/μ_L=4.00		
	Present	Elasticity	FEM	Present	Elasticity	FEM	Present	Elasticity	FEM
0.0	1.006459	1.000056	1.000282	1.000016	1.000016	1.000000	1.000016	1.000016	1.000439
-0.2	1.005707	0.999601	0.999717	0.991263	0.991265	0.992868	0.967659	0.966703	0.968709
-0.4	0.985236	0.979897	0.980357	0.947638	0.947678	0.949453	0.879157	0.876539	0.878389
-0.6	0.924693	0.920611	0.921240	0.862775	0.862838	0.864507	0.761803	0.757677	0.759228
-0.8	0.829478	0.826833	0.827449	0.755310	0.755382	0.756817	0.645773	0.640776	0.642078
-1.0	0.718468	0.716794	0.717374	0.645671	0.645740	0.647021	0.544476	0.539590	0.540793

Table 3 Comparison of the non-dimensional displacements $(u_z/h)\times 10^{-3}$ for three methods considered (a/h=1.00)

z/h	μ_U/μ_L=0.25			μ_U/μ_L=1.00			μ_U/μ_L=4.00		
	Present	Elasticity	FEM	Present	Elasticity	FEM	Present	Elasticity	FEM
0.0	-0.3453	-0.3429	-0.3389	-0.2223	-0.2255	-0.2254	-0.1615	-0.1635	-0.1595
-0.2	-0.2855	-0.2814	-0.2837	-0.2077	-0.2082	-0.2008	-0.1588	-0.1627	-0.1558
-0.4	-0.2375	-0.2333	-0.2256	-0.1903	-0.1908	-0.1933	-0.1524	-0.1563	-0.1533
-0.6	-0.2003	-0.1960	-0.1983	-0.1720	-0.1724	-0.1749	-0.1431	-0.1470	-0.1440
-0.8	-0.1731	-0.1687	-0.1609	-0.1543	-0.1548	-0.1572	-0.1318	-0.1358	-0.1321
-1.0	-0.1537	-0.1494	-0.1515	-0.1384	-0.1388	-0.1312	-0.1192	-0.1232	-0.1201

Table 4 Comparison of the non-dimensional normal stresses σ_z/q_0 for three methods considered (μ_U/μ_L=1.00)

z/h	a/h=0.01			a/h=1.00			a/h=2.00		
	Present	Elasticity	FEM	Present	Elasticity	FEM	Present	Elasticity	FEM
0.0	1.000000	1.000000	1.000269	1.000016	1.000016	1.000000	1.000037	1.0009049	1.000000
-0.2	0.003738	0.003738	0.004006	0.991263	0.991265	0.992868	1.002526	1.002535	0.999082
-0.4	0.000936	0.000936	0.000945	0.947638	0.947678	0.949453	0.995943	0.9959643	0.992586
-0.6	0.000416	0.000416	0.000419	0.862775	0.862838	0.864507	0.979703	0.979730	0.976476
-0.8	0.000234	0.000234	0.000235	0.755310	0.755382	0.756817	0.952106	0.952141	0.949032
-1.0	0.000150	0.000150	0.000145	0.645671	0.645740	0.647021	0.913754	0.913798	0.910919

Table 5 Comparison of the non-dimensional displacements $(u_z/h)\times10^{-3}$ for three methods considered (μ_U/μ_L=1.00)

z/h	*a/h*=0.01			*a/h*=1.00			*a/h*=2.00		
	Present	Elasticity	FEM	Present	Elasticity	FEM	Present	Elasticity	FEM
0.0	-21.1933	-21.2833	-21.4000	-0.2223	-0.2255	-0.2254	-0.1109	-0.1088	-0.1041
-0.2	-0.9533	-0.9543	-0.9818	-0.2077	-0.2082	-0.2068	-0.1074	-0.1079	-0.0996
-0.4	-0.4768	-0.4774	-0.4710	-0.1903	-0.1908	-0.1906	-0.1036	-0.1040	-0.0967
-0.6	-0.3177	-0.3182	-0.3107	-0.1720	-0.1724	-0.1749	-0.0994	-0.0998	-0.0924
-0.8	-0.2382	-0.2386	-0.2310	-0.1543	-0.1548	-0.1572	-0.0949	-0.0953	-0.0914
-1.0	-0.1904	-0.1909	-0.1933	-0.1384	-0.1388	-0.1312	-0.0903	-0.0907	-0.0893

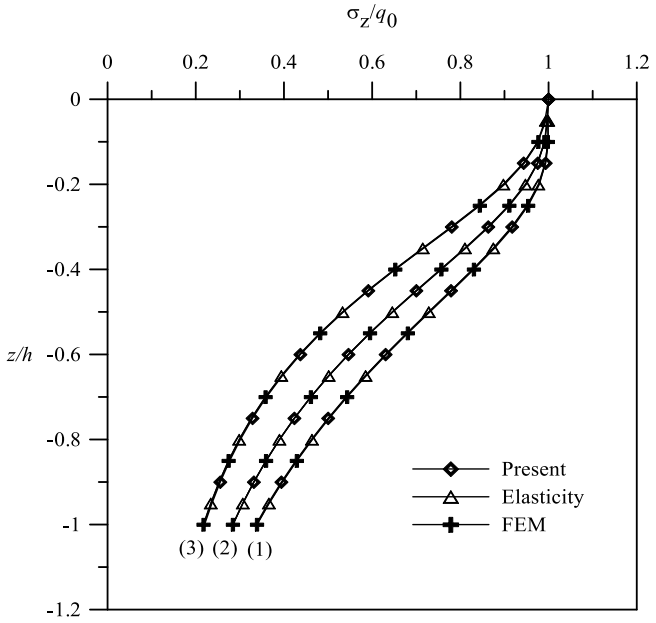

Fig. 6 Non-dimensional normal stress (σ_z/q_0) distribution in the FG layer through the thickness: (1) μ_U/μ_L=0.25; (2) μ_U/μ_L=1.00; (3) μ_U/μ_L=4.00 (*a/h*=0.5)

Tables 2 and 3 compare the non-dimensional normal stresses σ_z/q_0 and the non-dimensional vertical displacements u_z/h according to three methods considered for various μ_U/μ_L values, respectively. Here *a/h*=1.00 is selected. As seen in the tables, results show excellent agreement. Table 4 and 5 give the non-dimensional stresses σ_z/q_0 and the non-dimensional displacements u_z/h according to three methods considered for homogeneous layer by depending on the load length, respectively. Results are still in good agreement.

In Figs. 6 and 7, the non-dimensional stresses σ_z/q_0 and the non-dimensional vertical displacement u_z/h in the FG layer through the thickness for different μ_U/μ_L values and *a/h*=0.50 are given. As seen in the figures, the present method, the classical method and FEM are in excellent agreement. Normal stresses and vertical displacements decrease with increasing μ_U/μ_L ratio. This is expected because the upper part of the layer becomes stiffer when μ_U/μ_L increases.

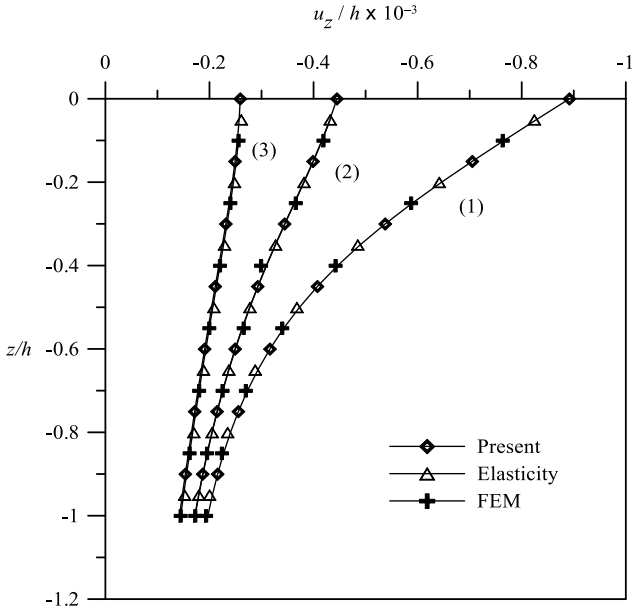

Fig. 7 Non-dimensional displacement (u_z/h) distribution in the FG layer through the thickness: (1) μ_U/μ_L=0.25; (2) μ_U/μ_L=1.00; (3) μ_U/μ_L=4.00 (a/h=0.5)

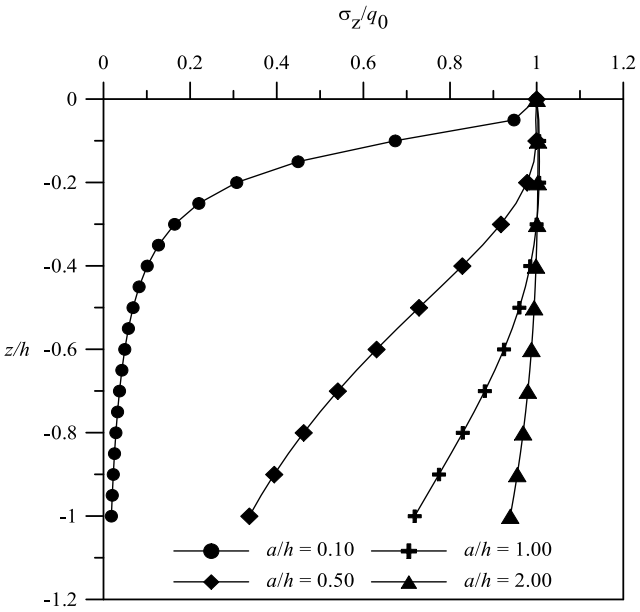

Fig. 8 Non-dimensional normal stress (σ_z/q_0) distribution in the FG layer through the thickness for different load lengths (μ_U/μ_L=0.25)

Figs. 8 and 9 give the non-dimensional stresses σ_z/q_0 for the FG layer depending on the load length. It can be still observed the results from three methods are in good agreement. For loads distributed over a smaller area, e.g., a/h=0.10, the normal stresses are decreased rapidly when $z \rightarrow -h$.

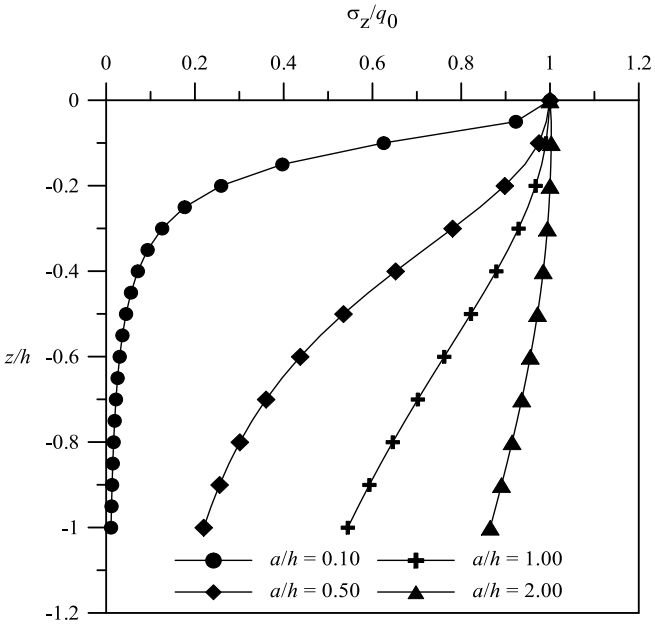

Fig. 9 Non-dimensional normal stress (σ_z/q_0) distribution in the FG layer through the thickness for different load lengths (μ_U/μ_L=4.00)

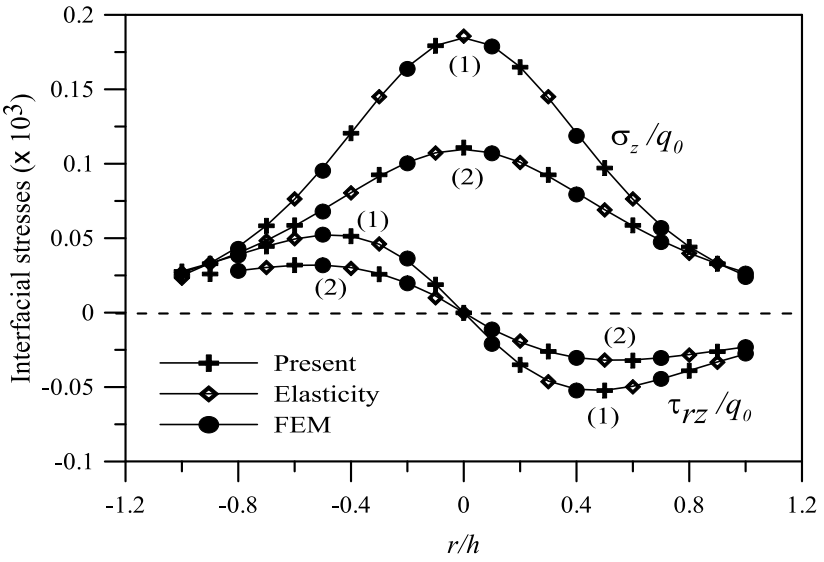

Fig. 10 Non-dimensional normal and shear stress distributions at the layer – half-space interface along the radial direction: (1) μ_U/μ_L=0.25; (2) μ_U/μ_L=4.00 (a/h=0.01)

Figs 10 and 11 show the non-dimensional normal and shear stresses at the layer – half-space interface along the radial direction with different μ_U/μ_L values. As expected, the normal and shear stresses both approaches to zero when $r/h \rightarrow \pm\infty$. Here, we can still observe that the results for three methods considered show excellent agreement. In addition, it can be seen from these figures when

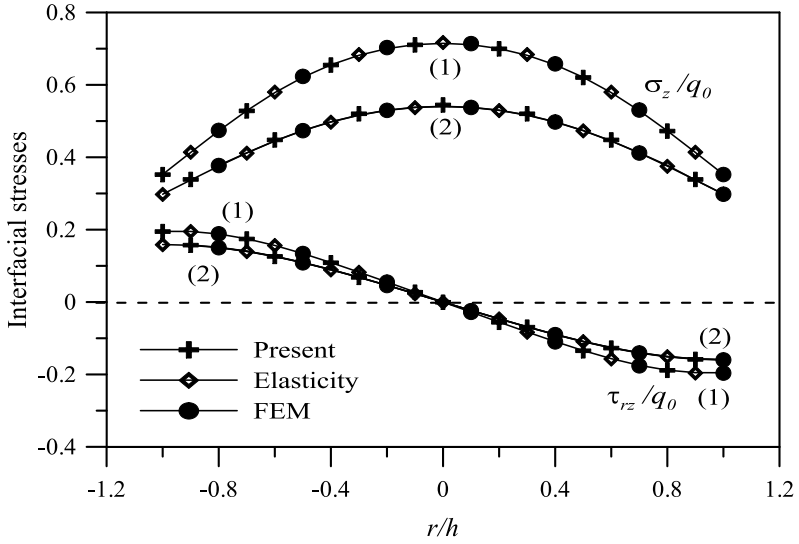

Fig. 11 Non-dimensional normal and shear stress at the layer – half-space interface along the radial direction: (1) μ_U/μ_L=0.25; (2) μ_U/μ_L=4.00 (a/h=1.00)

μ_U/μ_L increases, both shear and normal stresses decrease since upper part of the layer becomes stiffer compared to the lower part.

5. Conclusions

Elasto-static problem of a FG layer resting on elastic homogenous substrate under axisymmetric loading is studied by the stiffness matrix method. The FG layer is approximated into N-layer medium in which each layer is assumed to be homogeneous and isotropic with a different shear modulus. Results obtained are compared to those of the exact elasticity and the FE solutions. Numerical results for displacements and stresses are in excellent agreement. Although we used N homogeneous sublayer with different elastic moduli to represent the FG layer, it can be concluded that the stiffness matrix method gave satisfactory results, thus, the method can be safely applied to the problems of elastic media including FGMs.

References

Ai, Z.Y. and Cai, J.B. (2015), "Static analysis of Timoshenko beam on elastic multilayered soils by combination of finite element and analytical layer element", *Appl. Math. Model.*, **39**, 1875-1888.

Ai, Z.Y., Cheng, Y.C. and Zeng, W.Z. (2011), "Analytical layer-element solution to axisymmetric consolidation of multilayered soils", *Comput. Geotech.*, **38**, 227-232.

Ai, Z.Y. and Wang, L.J. (2015), "Axisymmetric thermal consolidation of multilayered porous thermoelastic media due to a heat source", *Int. J. Numer. Anal. Meth. Geomech.*, **39**, 1912-1931.

Ai, Z.Y. and Zeng, W.Z. (2012), "Analytical layer-element method for non-axisymmetric consolidation of multilayered soils", *Int. J. Numer. Meth. Eng.*, **86**, 533-545.

ANSYS 15 (2015), Swanson Analysis Systems.

Bahar, L.Y. (1972), "Transfer matrix approach to layered systems", *ASCE J. Eng. Mech. Div.*, **98**, 1159-1172.
Barik, S.P., Kanoria, M. and Chaudhuri, P.K. (2009), "Frictionless contact of a functionally graded half-space and a rigid base with an axially symmetric recess", *J. Mech.*, **25**(1), 9-18.
Bufler, H. (1971), "Theory of elasticity of a multilayered medium", *J. Elast.*, **1** 125-143.
Chen, W.T. (1971), "Computation of stresses and displacements in a layered elastic medium", *Int. J. Eng. Sci.*, **9**, 775-800.
Choi, H.J. and Thangjitham, S. (1991), "Stress analysis of multilayered anisotropic elastic media", *J. Appl. Mech.*, **58,** 382-387.
Iyengar, S.R. and Alwar, R.S. (1964), "Stresses in a layered half-plane", *ASCE J. Eng. Mech. Div.*, **90**, 79-96.
Oner, E., Yaylaci, M. and Birinci, A. (2015), "Analytical solution of a contact problem and comparison with the results from FEM", *Struct. Eng. Mech.*, **54**(4), 607-622.
Pagano, N.J. (1970), "Influence of shear coupling in cylindrical bending of anisotropic laminates", *J. Compos. Mater.*, **4**, 330-343.
Pindera, M.J. and Lane, M.S. (1993), "Frictionless contact of layered half-planes, Part I: Analysis", *J. Appl. Mech.*, **60**, 633-639.
Pindera, M.J. and Lane, M.S. (1993), "Frictionless contact of layered half-planes, Part II: Numerical results", *J. Appl. Mech.*, **60**, 640-645.
Rhimi, M., El-Borgi, S. and Lajnef, N. (2011), "A double receding contact axisymmetric problem between a functionally graded layer and a homogeneous substrate", *Mech. Mater.*, **43**(12), 787-798.
Small, J.C. and Booker, J.R. (1984), "Finite layer analysis of layered elastic materials using a flexibility approach. Part 1- Strip loadings", *Int. J. Numer. Meth. Eng.*, **20**, 1025-1037.
Small, J.C. and Booker, J.R. (1986), "Finite layer analysis of layered elastic materials using a flexibility approach. Part 2- Circular and rectangular loadings", *Int. J. Numer. Meth. Eng.*, **23,** 959-978.
Senjuntichai, T. and Rajapakse, R.K.N.D. (1995), "Exact stiffness method for quasi-statics of a multi-layered poroelastic medium", *Int. J. Solid. Struct.*, **32**(11), 1535-1553.
Sun, L. and Luo, F. (2008), "Transient wave propagation in multilayered viscoelastic media: theory, numerical computation and validation", *ASME J. Appl. Mech.*, **75**, 1-15.
Sun, L., Gu, W. and Luo, F. (2009), "Steady-State wave propagation in multilayered viscoelastic media excited by a moving dynamic distributed load", *ASME J. Appl. Mech.*, **76**, 1-15.
Sun, L., Pan, Y. and Gu, W. (2013), "High-order thin layer method for viscoelastic wave propagation in stratified media", *Comput. Meth. Appl. Mech. Eng.*, **257,** 65-76.
Liu, T.J., Ke, L.L., Wang, Y.S. and Xing, Y.M (2015), "Stress analysis for an elastic semispace with surface and graded layer coatings under induced torsion", *Mech. Bas. Des. Struct. Mach.*, **43**(1), 74-94.
Thangjitham, S. and Choi, H.J. (1991), "Thermal stress analysis of a multilayered anisotropic medium", *J. Appl. Mech.*, **58**, 1021-1027.
Wang, W. and Ishikawa, H. (2001), "A method for linear elasto-static analysis of multi-layered axisymmetrical bodies using Hankel's transform", *Comput. Mech.*, **27**, 474-483.

CC

Appendix A

The stiffness matrix of an elastic layer is given by

$$\left[\begin{array}{c|c} \mathbf{K}_{11}^{k} & \mathbf{K}_{12}^{k} \\ \hline \mathbf{K}_{21}^{k} & \mathbf{K}_{22}^{k} \end{array}\right] = \begin{bmatrix} k_{11} & k_{12} & k_{13} & k_{14} \\ k_{21} & k_{22} & k_{23} & k_{24} \\ k_{31} & k_{32} & k_{33} & k_{34} \\ k_{41} & k_{42} & k_{43} & k_{44} \end{bmatrix} \tag{A.1}$$

where

$$k_{11} = -\frac{s(2\mu+\lambda)(R-1)(2hs+Rsinh(2hs))}{R^2 - R^2 cosh(2hs) + 2h^2 s^2},$$

$$k_{12} = -\frac{s(2\mu R - \lambda R^2 + \lambda R + 4\mu h^2 s^2 - 2\mu R cosh(2hs) - \lambda R cosh(2hs) + \lambda R^2 cosh(2hs))}{R^2 - R^2 cosh(2hs) + 2h^2 s^2},$$

$$k_{13} = \frac{s(2\mu+\lambda)(Rsinh(hs)+hscosh(hs))(R-1)}{R^2 - R^2 cosh(hs)^2 + h^2 s^2}, \quad k_{14} = \frac{hs^2 sinh(hs)(2\mu+\lambda)(R-1)}{R^2 sinh(hs)^2 - h^2 s^2},$$

$$k_{21} = -\frac{\mu s(Rcosh(2hs) - R - R^2 cosh(2hs) + R^2 + 4h^2 s^2)}{R^2 - R^2 cosh(2hs) + 2h^2 s^2}, \quad k_{22} = \frac{\mu s(R+1)(2hs - Rsinh(2hs))}{R^2 - R^2 cosh(2hs) + 2h^2 s^2},$$

$$k_{23} = -\frac{\mu hs^2 sinh(hs)(R+1)}{R^2 sinh(hs)^2 - h^2 s^2}, \quad k_{24} = \frac{\mu s(Rsinh(hs) - hscosh(hs))(R+1)}{R^2 - R^2 cosh(hs)^2 + h^2 s^2},$$

$$k_{31} = \frac{s(2\mu+\lambda)(Rsinh(hs)+hscosh(hs))(R-1)}{R^2 - R^2 cosh(2hs) + h^2 s^2}, \quad k_{32} = -\frac{hs^2 sinh(hs)(2\mu+\lambda)(R-1)}{R^2 sinh(hs)^2 - h^2 s^2},$$

$$k_{33} = -\frac{s(2\mu+\lambda)(R-1)(2hs+Rsinh(2hs))}{R^2 - R^2 cosh(2hs) + 2h^2 s^2},$$

$$k_{34} = \frac{s(2\mu R - \lambda R^2 + \lambda R + 4\mu h^2 s^2 - 2\mu R cosh(2hs) - \lambda R cosh(2hs) + \lambda R^2 cosh(2hs))}{R^2 - R^2 cosh(2hs) + 2h^2 s^2},$$

$$k_{41} = \frac{\mu hs^2 sinh(hs)(R+1)}{R^2 sinh(hs)^2 - h^2 s^2}, \quad k_{42} = \frac{\mu s(Rsinh(hs) - hscosh(hs))(R+1)}{R^2 - R^2 cosh(hs)^2 + h^2 s^2}$$

$$k_{43} = \frac{\mu s(Rcosh(2hs) - R - R^2 cosh(2hs) + R^2 + 4h^2 s^2)}{R^2 - R^2 cosh(2hs) + 2h^2 s^2}, \quad k_{44} = \frac{\mu s(R+1)(2hs - Rsinh(2hs))}{R^2 - R^2 cosh(2hs) + 2h^2 s^2} \tag{A.2}$$

Appendix B

The stiffness matrix for a half space is given by

$$\left[\mathbf{K}_{11}^{k}\right]=\begin{bmatrix} k_{11} & k_{12} \\ k_{21} & k_{22} \end{bmatrix} \tag{B.1}$$

where

$$k_{11}=\frac{s\left(2\mu+\lambda\right)\left(R-1\right)}{R\,sign\left(s\right)},\quad k_{12}=-\frac{s\left(2\mu+\lambda-\lambda R\right)}{R},$$

$$k_{21}=-\frac{\mu s(R-1)}{R\,sign(s)^{2}},k_{22}=\frac{\mu\,abs\left(s\right)\left(R+1\right)}{R} \tag{B.1}$$